Effect of co-electrodeposited Cu-Zn-Sn precursor compositions on sulfurized CZTS thin films for solar cell

M. I. Khalil[a], R. Bernasconi[a], S. Ieffa[a], A. Lucotti[b], A. Le Donne[c], S. Binetti[c], L. Magagnin[a,*]

[a] Dipartimento di Chimica, Materiali e Ing. Chimica Giulio Natta, Politecnico di Milano, Via Mancinelli 7, 20131, Milano (Italy)

[b] Dipartimento di Chimica, Materiali e Ing. Chimica Giulio Natta, Politecnico di Milano, Piazza Leonardo da Vinci 32, 20133, Milano (Italy)

[c] Department of Materials Science and Solar Energy Research Centre (MIB-SOLAR), University of Milano- Bicocca, Via Cozzi 53, 20125, Milano (Italy)

* Corresponding author: luca.magagnin@polimi.it
Phone: +390223993124, fax: +390223993180

Introduction

The quaternary compound Cu_2ZnSnS_4 (CZTS) based thin film solar cells are considered promising possible alternative to Cu (InGa) Se_2 (CIGS) based thin film solar cells due to their abundant constituent materials, suitable direct band gap of 1.4-1.5 eV and high absorption coefficient over 10^4 cm^{-1} [1] as well as good theoretical power conversion efficiency around 32% (based on Shockley–Queisser photon balance calculations [2]). Up to now, CIGS based thin film solar cells showed greater performance both in laboratory and industry scale. However, CIGS contains rare earth materials like indium and gallium as well as selenium. Moreover, In and Ga are also used in display technology. Considering production on large scale of thin film solar cells, CZTS has a potential to replace CIGS where In, Ga and Se are substituted by zinc (Zn), tin (Sn) and sulphur (S). Highest conversion efficiency of CZTS thin film solar cell has reached 9.2 % (in case of pure sulphide) [3], while sulfo-selenide (CZTSSe) thin film solar cell conversion efficiency reached 12.6% [4].

CZTS has been fabricated by different vacuum based techniques like sputtering, evaporation, pulsed laser deposition etc. On the other hand, non-vacuum based techniques

like electrodeposition, the sol-gel method, a solution-particle approach, screen printing etc. have also been employed to fabricate CZTS thin film solar cells. Though majority of the CZTS thin film solar cells have been fabricated by vacuum based techniques, nowadays non-vacuum based techniques have gained attraction since they provide a low cost deposition. Electrodeposition is one of the potentially suitable non-vacuum based techniques for the fabrication of CZTS thin film solar cells. Electrodeposition provides 1) high quality film with low capital investment 2) low temperature growth 3) automatic purification of the material during electrodeposition 4) easier to deposit large area with multi components etc. Usually electrodeposition processes for the fabrication of CZTS thin films can be divided into two categories; 1) Direct electrodeposition of Cu, Zn, Sn and S from single electrolyte and subsequent annealing in sulfur atmosphere 2) Electrodeposition of Cu, Zn and Sn from single electrolyte or different electrolytes to form stacked layers (Zn/Sn/Cu or Sn/Zn/Cu) and later annealing in sulfur atmosphere in both cases. It is very difficult to deposit homogenous and compact films of Cu, Zn, Sn and S from single electrolyte, as the reduction potential gap among these metal ions is considerably large. Moreover, it has been reported that sulfur containing precursor films do not increase the grain size (which is related to efficiency) after sulfurization, though it has been done by sputtering [5]. For this reason electrodeposition of Cu, Zn and Sn followed by annealing in sulfur atmosphere has been preferred by researchers. Since there are some issues in case of stacked metallic precursors of Cu, Zn and Sn which have been published in our report elsewhere [6], simultaneous electrodeposition of Cu, Zn and Sn from single electrolyte has been preferred.

CZTS has been fabricated by several groups over the past years through electrodeposition - annealing route. In 2008, Scragg et al. first reported sequential electrodeposition method for CZTS thin film with 0.8% power conversion efficiency [7]. In this method, stacked metal layers of Cu/Sn/Zn were deposited on a Mo/SLG (sodalime glass) substrate sequentially using a three-electrode system and later annealed at 550^0C with sulfur atmosphere. In 2009 Araki et al. demonstrated CZTS thin film from stacked precursor and co-electroplated precursor with 0.98% and 3.16% power conversion efficiency [8, 9]. At the same time, Ennaoui et al. fabricated CZTS thin film from co-electroplated Cu-Zn-Sn precursor with 3.4% power conversion efficiency [10]. Araki et al. fabricated their film through annealing in sulfur atmosphere whereas Ennaoui et al. fabricated their films through annealing in H_2S atmosphere. In 2010 again Scragg et al. demonstrated CZTS thin films from stacked precursor of Cu-Zn-Sn through annealing in sulfur atmosphere with 3.2% power conversion efficiency [11]. In 2012 Ahmed et al. from IBM got substantial success in preparing CZTS thin film from stacked precursor of Cu-Zn-Sn with 7.3% power conversion efficiency [12]. They also sulfurized their film in elemental sulfur atmosphere. They reduced the sulfurization time from 2 hours to 5-15 mins with respect to previous reports. Point to be noted, before sulfurization they soft (pre) annealed the precursor at 350^0C for 30 minutes to produce homogeneous CuZn and CuSn alloy. Recently Lin at al. showed the mechanistic aspects of preheating effects of electrodeposited metallic stacked precursor with 5.6% power conversion efficiency [13]. Also Jiang et al. Fabricated CZTS thin films solar cells from stacked metallic precursor with 8% power conversion efficiency where they pre-annealed the precursors at lower temperature with longer durations [14]. This is the highest power conversion efficiency of CZTS thin films solar cell via electrodeposition-annealing route up to our knowledge. Li et al. fabricated CZTS thin film from co-electroplated Cu-Zn-Sn precursor with 3.62% power conversion efficiency [15].

In this work we studied the effect of precursor composition of Cu-Zn-Sn on the sulfurized films where precursors have been prepared from novel electrolyte formulation [6]. After co-electroplating, three precursor of Cu-Zn-Sn with different compositions have been annealed at 550^0C for 2 hours with 20^0C/minutes ramping rate in elemental sulfur atmosphere in the presence of reduced flow of N_2.

Experimental methods

Electrodeposition was carried out galvanostatically in a conventional electrochemical cell assembly. Mo coated sodalime glass (SLG) with an 2×1 cm^2 exposed area was used as a working electrode and graphite was used as inert counter electrode. Before the deposition, Mo coated SLG substrates were cleaned with acetone, washed in distilled water and later dried in N_2 atmosphere. Our electrolyte bath, which has been published elsewhere [6], contains 0.016 M $CuSO_4 \cdot 5H_2O$, 0.072 M $ZnSO_4 \cdot 7H_2O$, 0.037 M $Na_2SnO_3 \cdot 3H_2O$, 0.60 M $K_4P_2O_7$ and additives. Different compositions of the precursor films of Cu-Zn-Sn have been prepared with the help of various current densities and stirring of the electrolyte. After electroplating, precursors were annealed in a quartz tube furnace at 550^0C with 20^0C/minute ramping rate in sulfur atmosphere in the presence of a small flow of N_2. The crystallographic phase of as deposited Cu-Zn-Sn precursors and annealed thin films was analyzed with the help of X-ray diffractometer (XRD, Philips X-pert MPD with CuKα = 1.5406Å). Evolution of the surface morphology and the composition of the as deposited precursors and sulfurized films were analysed by scanning Electron Microscopy (Model Zeiss EVO 50) equipped with an energy dispersive X-ray analyzer (EDS) Oxford instrument (Model 7060). Raman measurements were carried out at room temperature with a Jasco Ventuno micro-Raman system in backscattering configuration, equipped with a cooled charge-coupled device camera (operating T = -65°C) and a He-Ne laser (excitation wavelength of 632.8 nm). The laser power density was chosen to generate the best signal-to-noise ratio without broadening or shift of the Raman peaks due to local heating (objective 20X)

Results and discussion

X-Ray diffractograms of as deposited precursor are shown in Fig. 1.

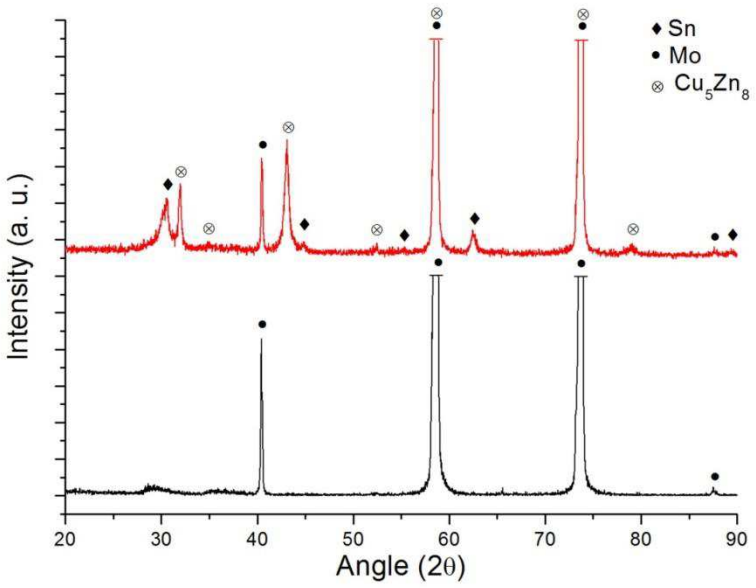

Figure 1. XRD patterns of as deposited precursor and Mo substrate

From figure 1 it is evident that the as deposited Cu-Zn-Sn precursors are composed of pure Sn (JCPDS 86-2265) and Cu_5Zn_8 (JCPDS card 25-1228) phases. Here, some of the Mo peaks have been cut due to their excessive intensity. The formation of some other peaks such as pure Cu, pure Zn, CuZn, Cu_6Sn_5 have been reported in other literature [9, 16, 17] in case of co-electrodeposition of Cu-Zn-Sn in acidic electrolytes. As, Zn and Sn do not form any intermetallic compounds, there have been no report of ZnSn phases in the literature. Crystallographic phases of as deposited precursors of Cu-Zn-Sn depend on many variables like type of precursors (co-electrodeposited/stacked layers), composition of precursors, source materials in electrolyte, kind of electrolyte used (acidic/alkaline) etc. It has been reported that Cu-poor, Zn-rich precursor is favourable for good CZTS films [18, 19]. R. Schurr et al. reported that variations of precursor compositions and precursor binary phases have great influence on the formation reactions of products and Kesterite [20]. In their cases, they had Cu_3Sn and CuZn phases on Cu-rich sample and Cu_6Sn_5 and Sn phases on Cu-poor/ stoichiometric samples. In this study, three samples with different precursor compositions ranging from Cu-poor, Zn-rich to Cu-rich, Zn-poor have been analyzed. In all the cases we observed Cu_5Zn_8 and pure Sn phases.

TABLE I. As deposited precursors composition

Sample No.	Cu (at. %)	Zn (at. %)	Sn (at. %)	Cu/(Zn + Sn)	Zn/Sn
(i)	47.70	28.66	23.64	0.91	1.21
(ii)	46.52	27.26	26.22	0.87	1.04
(iii)	56.42	17.13	26.44	1.29	0.64

After electroplating, Cu-Zn-Sn precursors have been sulfurized in a quartz tube furnace with 20^0C/ minutes ramping rate at 550^0C with 25-30 mg elemental sulfur environment for 2 hours with small flow of N2. It has been shown in our previous studies that low ramping rate (2^0C/ minutes) does not improve the film quality rather create some secondary

phases as CZTS is metastable [6]. Consequently 20^0C/ minutes heating rate has been used during sulfurization in the present work. The average composition ratios of as deposited and sulfurized films were measured by EDS and are shown in Table 1 and Table 2. Here, (i) and (ii) are Cu-poor sample and sample (iii) is Cu-rich. Due to the volatility of Zn, Sn (in the form of SnS) and S during sulfurization, precursor compositions play a vital rule to form CZTS during sulfurization process [21].

TABLE II. Elemental composition of CZTS films

Sample No.	Cu (at. %)	Zn (at. %)	Sn (at. %)	S (at. %)	Cu/ (Zn + Sn)	Zn/Sn	S/metal
(i)	24.94	12.55	11.98	50.54	1.01	1.04	1.02
(ii)	25.48	11.15	13.40	49.97	1.04	0.83	0.99
(iii)	27.17	9.51	13.72	49.61	1.17	0.69	0.98

Fig. 2 shows the SEM morphology of three different precursors with same magnification, where the film appears very compact and well adherent.

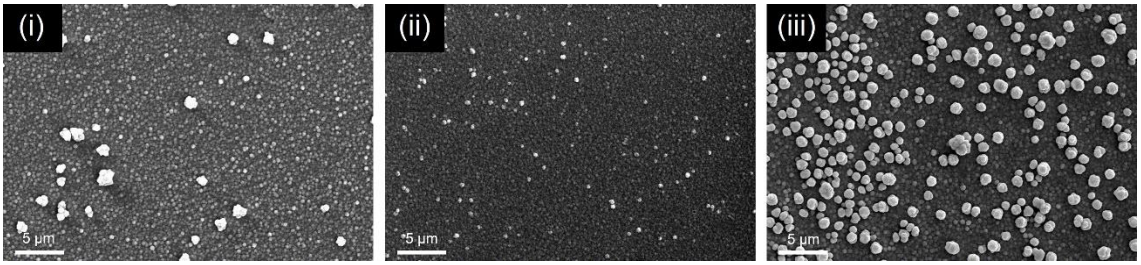

Figure 2. SEM morphologies of as deposited precursor of co-electroposited Cu-Zn-Sn films

White zones in the Fig. 2 are Cu rich (near about 2-5% deviation from average Cu composition in the film) which has been confirmed by EDS measurement. Different compositions of the precursors have been obtained with the application of different current densities and stirring of the electrolyte. Average film thickness was about 600-700 nm. Fig.3 shows the XRD patterns of the films after sulfurization of the three different precursors.

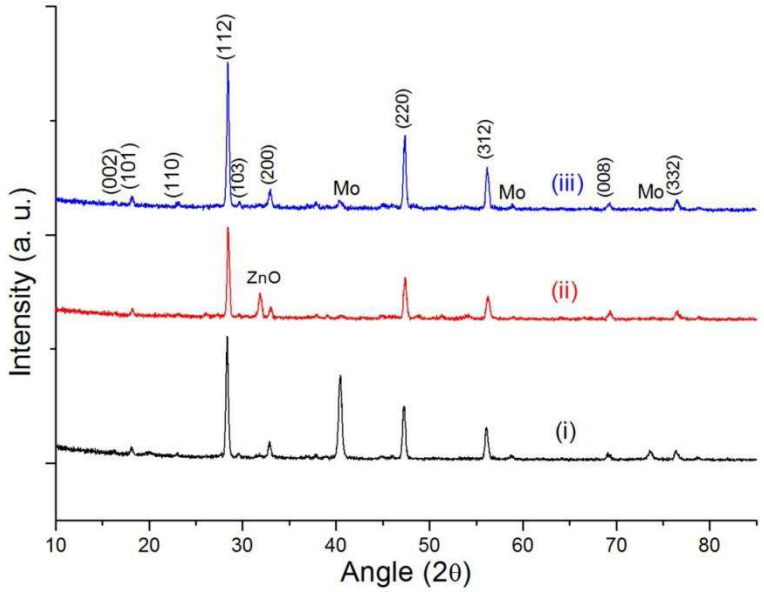

Figure 3. XRD patterns of sulfurized films

All XRD patterns of sulfurized films correspond to the peak of the Kesterite structure of CZTS (JCPDS card 26-0575) with dominant peak at 28.53^0 diffraction angle which was commonly acknowledged by others. In the case of (ii) Cu/(Zn+Sn) = 0.87; Zn/Sn = 1.04, a strong peak of ZnO was observed,probably connected to improper conditions during sulfurization step.

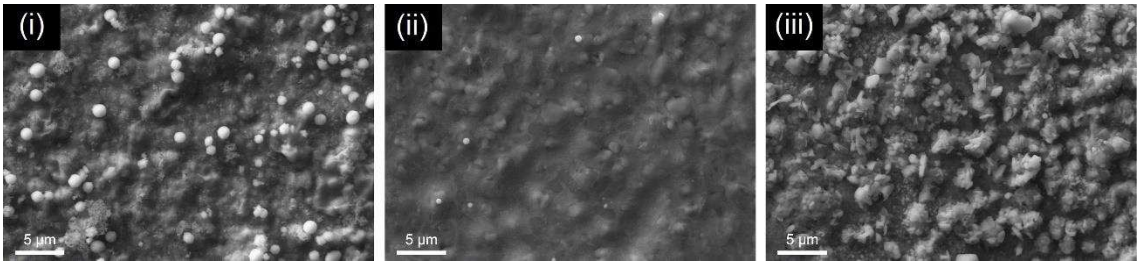

Figure 4. Surface morphology of the different films after sulfurization

Fig. 4 shows the SEM morphology of the surface of the films after sulfurization, which looks compact and smooth without any void or crevices. It is clear from the Table 2 that sample (i) Cu/(Zn+Sn) = 0.91; Zn/Sn = 1.21 has better compositional ratio (Cu: 24.94; Zn: 12.55; Sn: 11.98; S: 50.54) with respect to others two. Loss of Zn and Sn during sulfurization is also visible from Table 2 which justifies the findings of other research groups. For this reason, it is important to control the precursor composition to minimize the loss of Zn and Sn during sulfurization. However, there is not that much deviation of the S / Metal ratio in all three samples.

XRD result is not well enough to justify the presence of CZTS in the films as the peaks of ZnS and Cu_2SnS_3 are very close to CZTS. Hence samples were further characterized by using Raman spectroscopy. Fig. 5 shows the Raman spectra on sulfurized films.

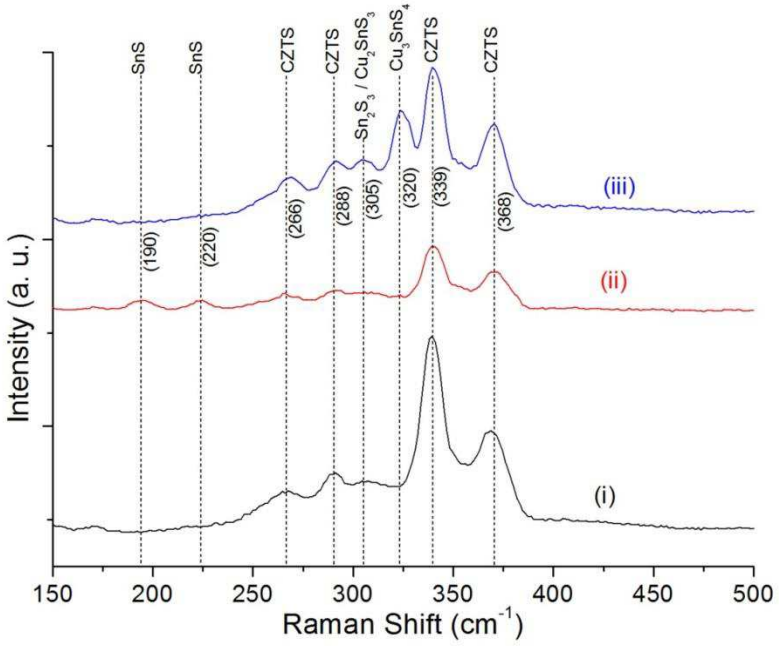

Figure 5. Raman spectra of the different sulfurized films

All samples (i. ii, iii) show the typical CZTS peaks at Raman shift 266 cm^{-1}, 288 cm^{-1}, 339 cm^{-1}, 368 cm^{-1}, with a significant commonly acknowledged strong peak at 339 cm^{-1} [12, 22, 23]. If we compare the Raman spectra of the three sulfurized films, we can observe in the case of sample (ii) the presence of SnS (190 cm^{-1}, 220 cm^{-1}), Sn_2S_3/ Cu_2SnS_3 (304,305 cm^{-1}) peaks and in the case of sample (iii) the presence of Sn_2S_3/ Cu_2SnS_3 (304 cm^{-1},305 cm^{-1}), Cu_3SnS_4 (320 cm^{-1}) peaks. Conversely, only small Raman peaks of Sn_2S_3/ Cu_2SnS_3 (304 cm^{-1},305 cm^{-1}) are visible in the case of sample (i). Those Raman peaks are in agreement with the existing literatures [23, 24, 25]. Peaks of secondary phases are probably connected with the incomplete reaction path of CZTS as Zn content on those two samples is less with respect to sample (i). Moreover, from figure 5 it is evident that sample (i) has very strong Raman peaks of CZTS with respect to the peaks of other phases (SnS, Sn_2S_3, Cu_2SnS_3, Cu_3SnS_4) which justifies compositional analysis by the EDS measurements.

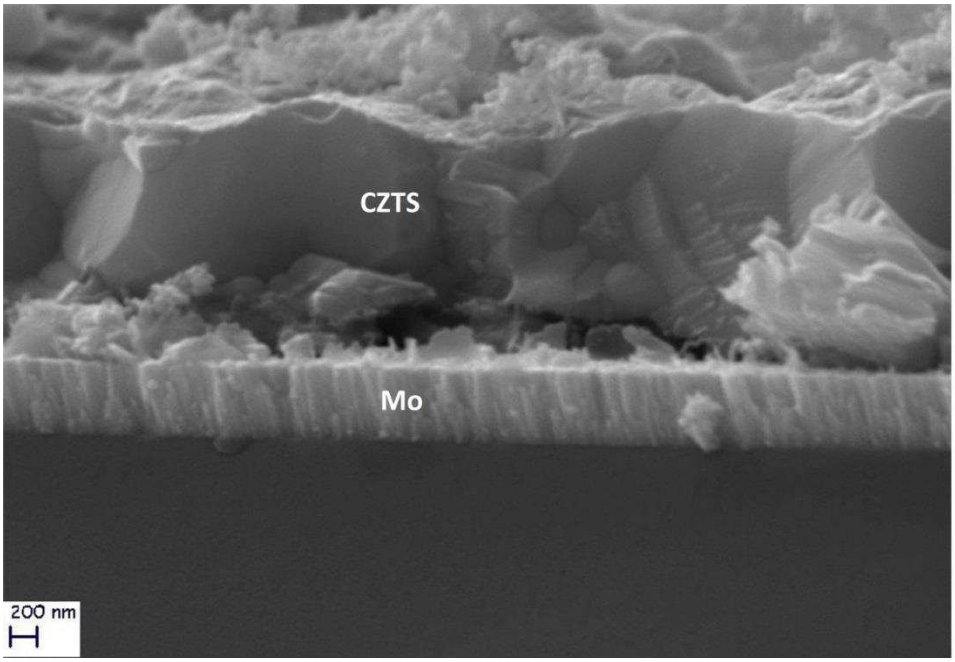

Figure 6. Cross sectional image of sulfurized film (i).

Fig. 6 shows the cross-sectional image of the sulfurized film (i), which looks very well formed and the CZTS obtained appears crystalline. It is shown in the figure that CZTS possess bimodal distribution of grains: smaller grains are located near the interface of Mo and larger grains at the top of the CZTS.

Conclusions

CZTS thin films from co-electrodeposited precursors of Cu-Zn-Sn with different compositions were successfully prepared via electrodeposition-annealing route and investigated. Results of different characterization methods show that in order to get well formed CZTS with minimum secondary phases, very careful control over precursor compositions is needed in order to eliminate the losses of Zn and Sn during sulfurization. In these studies good quality Kesterite CZTS films are obtained in case of Cu-poor, Zn-rich precursor with Cu/(Zn+Sn) = 0.91; Zn/Sn = 1.21, near to the stoichiometric composition of the elements after sulfurization.

References

1. K. Ito and T. Nakazawa, *Jpn. J. Appl.Phys.*, **1** (27), 2094 (1988).
2. W. Shockley and H.J. Queisser, *J. App. Phys.*,**32**,510 (1961).
3. T. Kato, H. Hiroi, N. Sakai, S. Muraoka and H. Sugimoto, 27th EU PVSEC, 2012,http://dx.doi.org/10.4229/27thEUPVSEC2012-3CO.4.2.
4. W. Wang , M. T. Winkler , O. Gunawan , T. Gokmen , T. K. Todorov ,Y. Zhu and D. B. Mitzi, *Adv. Energy Mater.*,**4**, 1301465 (2014).
5. C. Platzer-Björkman, J. Scragg, H. Flammersberger, T. Kubart and M. Edoff, *Sol. Energy Mater. Sol. Cells*, **98**, 110 (2012).

6. M. I. Khalil, R. Bernasconi and L. Magagnin,*Electrochim. Acta*, **145**, 154 (2014).
7. J. J. Scragg, P. J. Dale, L. M. Peter, G. Zoppi and I. Forbes, *Phys. Status Solidi B*, **9**, 1772 (2008).
8. H. Araki, Y. Kubo, A. Mikaduki, K. Jimbo,W. S. Maw, H. Katagiri, M. Yamazaki, K. Oishi and A. Takeuchi, *Sol. Energy Mater. Sol. Cells*, **93**, 996 (2009).
9. H. Araki, Y. Kubo, K. Jimbo,W. S. Maw, H. Katagiri, M. Yamazaki, K. Oishi and A. Takeuchi, *Phys. Status Solidi C*, **6** (5), 1266 (2009).
10. A. Ennaoui, M. Lux-Steiner, A. Weber, D. Abou-Ras, I. Kötschau, H. W. Schock, R. Schurr, A. Hölzing, S. Jost, R. Hock, T. Voß, J. Schulze and A. Kirbs, *Thin Solid Films*, **517**, 2511 (2009).
11. J. J. Scragg, D. M. Berg and Phillip J. Dale, *J. Electroanal. Chem.*, **646**, 52 (2010).
12. S. Ahmed, K. B. Reuter, O. Gunawan, L. Guo, L. T. Romankiw and H. Deligianni, *Adv. Energy Mater.*, **2**, 253 (2012).
13. Y. Lin, S. Ikeda, W. Septina, Y. Kawasaki, T. Harada and M. Matsumura, *Sol. Energy Mater. Sol. Cells*, **120**, 218 (2014).
14. F. Jiang, S. Ikeda, T. Harada and M. Matsumura, *Adv. Energy Mater.*, **4**, 1301381 (2014).
15. Y. Li, T. Yuan, L. Jiang, Z. Su and F. Liu, *J. Alloys Compd.*, **610**, 331 (2014).
16. K. V. Gurav, S. M. Pawar, S. W. Shin, M. P. Suryawanshi, G. L. Agawane, P. S. Patil,J. Moon, J. H. Yun andJ. H. Kim, *Appl. Surf. Sci.*, **283**, 74 (2013).
17. X. He, H. Shen, W. Wang, J. Pi, Y. Hao and X. Shi, *Appl. Surf. Sci.*, **282**, 765 (2013).
18. T. Kobayashi, K. Jimbo, K. Tsuchida, S. Shinoda, T. Oyanagi and H. Katagiri, *Jpn. J. Appl. Phys.*, **44**, 783 (2005).
19. H. Katagiri, *Thin Solid Films*, **426**, 480 (2005).
20. R. Schurr, A. Holzing, S. Jost, R. Hock, T. Voβ, J. Schulze, A. Kirbs, A. Ennaoui, M. Lux-Steiner, A. Weber, I. Kotschau and H. W. Schock, *Thin Solid Films*, **517**, 2465 (2009).
21. J. J. Scragg, T. Ericson, T. Kubart, M. Edo, and C. Platzer-Bjorkman, *Chem. Mater.*, **23**, 4625 (2011).
22. S. Marchionna, P. Garattini, A. Le Donne, M. Acciarri, S. Tombolato and S. Binetti, *Thin Solid Films*, **542**, 114 (2013).
23. P. A. Fernandes, P. M. P. Salome, A. F. Sartori, J. Malaquias, A. F. Da Cunha, B. Schubert, J. C. Gonzalez and G. M. Ribeiro, *Sol. Energy Mater. Sol. Cells*, **115**, 157 (2013).
24. P. A. Fernandes, P.M. P. Salome and A. F. Da Cunha, *J. Alloys Compd.*, **509**, 7600 (2011).
25. A. Fairbrother, X. Fontané, V. Izquierdo-Roca, M. Espíndola-Rodríguez, S. López-Marino, M. Placidi, L. Calvo-Barrio, A. Pérez-Rodríguez and E. Saucedo, *Sol. Energy Mater. Sol. Cells*, **112**, 97 (2013).